An Inversion Method for Measuring β in Large Redshift Surveys

Stephen D. Landy

Department of Physics, College of William and Mary, Williamsburg, VA 23187-8795, USA

landy@physics.wm.edu

and

Alexander S. Szalay

Department of Physics and Astronomy, The Johns Hopkins University, Baltimore, MD 21218, USA

ABSTRACT

A precision method for determining the value of $\beta = \Omega_m^{0.6}/b$, where b is the galaxy bias parameter, is presented. In contrast to other existing techniques that focus on estimating this quantity by measuring distortions in the redshift space galaxy-galaxy correlation function or power spectrum, this method removes the distortions by reconstructing the real space density field and determining the value of β that results in a symmetric signal. To remove the distortions, the method modifies the amplitudes of a Fourier plane-wave expansion of the survey data parameterized by β. This technique is not dependent on the small-angle/plane-parallel approximation and can make full use of large redshift survey data. It has been tested using simulations with four different cosmologies and returns the value of β to ± 0.031, over a factor of two improvement over existing techniques.

Subject headings: cosmological parameters—galaxies:distances and redshifts—galaxies:statistics—large-scale structure of the universe— methods:data analysis

1. Introduction

One of the principal goals of the current large redshift surveys, such as the Two-Degree Field (2dF) and Sloan Digital Sky Surveys (SDSS), is an improved estimation of the total mass density parameter Ω_m. A highly accurate measurement of Ω_m, along with measurements of the acoustic peaks in the CMB and the deceleration parameter q_o from distant

supernovae, should enable cosmologists to pin down the global geometry of the Universe and infer the value of Ω_λ, the vacuum energy density.

As is well-known, the redshift of a galaxy represents the sum of the galaxy's redshift distance, which depends upon cosmology, and its radial peculiar velocity. Therefore, raw redshift distance measurements are contaminated with the galaxies' radial peculiar velocities. Consequently, galaxy redshift survey statistical measures such as the two-point galaxy correlation function contain distortions due to the existence of galaxy peculiar velocities.

On large-scales in the linear regime, the galaxy peculiar velocities can be identified with fractional perturbations in the Hubble ratio $\Delta H/H$ due to fluctuations in the matter density field $\Delta\rho/\rho$, with $\Delta H/H \propto \Omega_m^{0.6}\Delta\rho/\rho$.[1] The peculiar velocities and resultant redshift distortions are statistical and by utilizing measures of the galaxy mass field, such as the galaxy-galaxy correlation function, together with the relation above, the distortions can be modeled and exploited as a way to measure Ω_m.

Since Ω_m is estimated using distortions in the galaxy correlation function or power spectrum and it is believed that galaxy formation is biased with respect to the underlying total mass field, what is actually measured is the parameter $\beta = \Omega_m^{0.6}/b$, where b is the bias in galaxy clustering with respect to the underlying mass field. Although somewhat problematic, this holds for any method that relies on the clustering of luminous matter to estimate a dynamical measure of the total mass field.

1.1. Kaiser's Method

The utility of using distortions in the galaxy redshift space correlation function to measure β in the linear regime was developed in detail by Kaiser (1987), although its use was anticipated by others (see Sargent & Turner 1977; Peebles 1980 §76). In this seminal work, Kaiser's unique contribution was in showing that the anisotropies generated by these radial peculiar velocities could be modeled as redshift space density enhancements in the underlying mass field.

Following Kaiser's lead, let us take a plane wave density fluctuation

$$\Delta_r(\mathbf{r}) = \Delta_k \cos(\mathbf{k}\cdot\mathbf{r} + \theta) \tag{1}$$

in real space. This real space plane wave fluctuation maps to redshift space in the following simple way,

[1]Assuming $\Omega_\lambda = 0$. Otherwise $\Omega_m^{0.6} \to \Omega_m^{0.6} + \frac{\Omega_\lambda}{70}(1 + \frac{\Omega_m}{2})$ (see Lahav *et al.* 1991)

$$\Delta_s(\mathbf{r}) = \Delta_r(\mathbf{r})[1 + \frac{\Omega_m^{0.6}}{b}\cos(\hat{\mathbf{k}}\cdot\hat{\mathbf{r}})^2] \tag{2}$$

or

$$\Delta_s(\mathbf{r}) = \Delta_r(\mathbf{r})(1 + \beta\mu^2) \tag{3}$$

where $\mu = \cos(\hat{\mathbf{k}}\cdot\hat{\mathbf{r}})$ is the cosine of the angle between the normed wavevectors $\hat{\mathbf{k}}$ and the line-of-sight $\hat{\mathbf{r}}$, Δ_s is the redshift space density, and $\beta = \Omega_m^{0.6}/b$. In the limit of small angular separations, the distortions in the redshift space power spectrum $P_s(\mathbf{k})$ are given by

$$P_s(\mathbf{k}) = P_r(\mathbf{k})(1 + \beta\mu^2)^2 \tag{4}$$

where $P_r(\mathbf{k})$ is the real space power spectrum. This limit is also known as the plane-parallel or distant observer approximation. Since the distortions contain powers of μ^2 and μ^4, they appear as a combination of quadrupole and hexadecapole distortions in $P_s(\mathbf{k})$. As Kaiser went on to note, it seemed more practical to find a way to determine β by using this result to calculate distortions in the redshift space correlation function, the correlation function being the Fourier transform of the power spectrum.

2. Difficulties in Measuring the Distortions

Traditionally, the approach to measuring distortions in the correlation function has been to decompose it in two-dimensions, where the two axes correspond to the directions parallel (π) and perpendicular (r_p) to the line-of-sight to a pair of galaxies. The line-of-sight direction has been taken to be the direction of the center-of-mass (Peebles 1980) or the half-angle (Landy, Szalay, & Broadhurst 1998; Hamilton 1992) between the pair. The resulting correlation function is denoted by $\xi_z(r_p, \pi)$. This decomposition for the correlation function for the simulation data is shown in Figure 1 on the following page.

However, measuring β from distortions in the correlation function has proven difficult for several reasons. Firstly, as evident in Figure 1, the distortions at small separations are due to galaxy pairwise velocities in the non-linear regime. These distortions are of an opposite sense than those due to large-scale linear infall. Whereas the latter cause a compression in the correlation function along the line-of-sight, the non-linear distortions create an expansion. Therefore, they are competing effects and errors in their measurement may be positively correlated when both are estimated simultaneously. Secondly, each of these distortions affect the correlation function in terms of convolutions. Convolutions are troublesome since it is the unknown underlying function convolved with the kernel that is actually estimated. And, since the distortions enter in the radial direction only, calculations of the expected

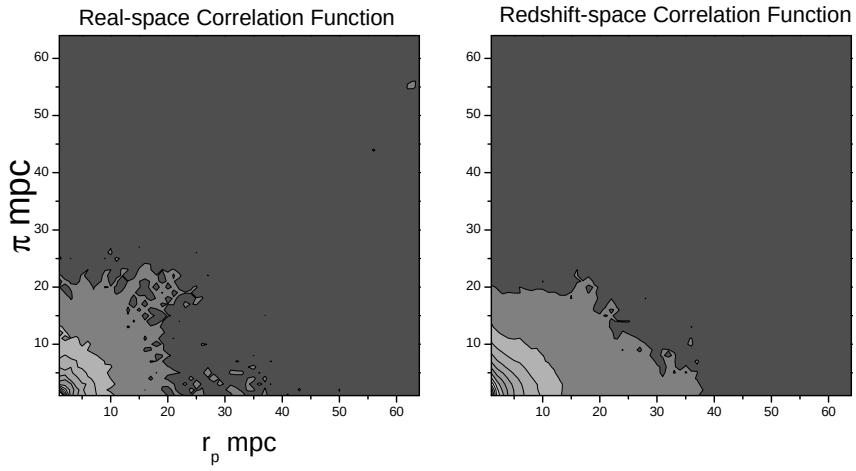

Fig. 1.— *The real and redshift space correlation functions from one of the simulations. The expansion in the redshift space function at small separations along the π-axis is due to the small-scale non-linear pairwise velocity dispersion. The compression at larger separations is due to large-scale infall, which is a function of β.*

correlation function given a particular power spectrum are extremely complicated and involve an integration over the spectrum itself, whose value may be only weakly constrained. For example, Kaiser's original paper derives the correlation function for the case of linear infall for *just the line-of-sight direction* as:

$$\xi_z(0,r_p) = 4\pi \int_0^\infty dk k^2 P_r(k) \Bigg[\sin(kr) \left\{ \frac{1}{kr} + 2\Omega^{0.6} \frac{[(kr)^2-2]}{(kr)^3} + \Omega^{1.2} \frac{[(kr)^4 - 12(kr)^2 + 24]}{(kr)^5} \right\} + \cos(kr) \left\{ \frac{4\Omega^{0.6}}{(kr)^2} + \Omega^{1.2} \frac{[4(kr)^2 - 24]}{(kr)^4} \right\} \Bigg] \quad (5)$$

with $b = 1$. And thirdly, unless measurements of the correlation function are restricted to small angular separations for the galaxy pairs (the distant observer approximation), the expected distortions in the correlation function become even more complex. The complete problem in the case of wide-angles was recently solved in Szalay, Matsubara, & Landy (1998) and computer algebra was needed to keep track of the numerous terms.

Attempting to measure the distortions using the power spectrum rather than the correlation function has also proven problematic. The basic intractability of this problem mainly results from the fact that radial distortions are not translationally invariant. The simple form for the distortions $P_s(\mathbf{k}) = P_r(\mathbf{k})(1+\beta\mu^2)^2$ given by Kaiser is only valid in the limit of small angles. Even with today's redshift surveys, this severely limits the amount of data that can be used in an analysis. A full decomposition of the distortions in the power spectrum in the case of wide-angles again results in very complex equations and requires a model for

the underlying power spectrum since the distortions cross-correlate Fourier modes on very different scales.

Many researchers have been working over the last two decades on developing clever and robust methods to model the distortions and these methods have been based principally upon one of three approaches. The first involves measuring the ratio of the angle-averaged redshift space to real space power spectrum or correlation function (see Fry & Gaztañaga 1994; Peacock & Dodds 1994; Baugh 1996; Loveday *et al.* 1996; Tadros & Efstathiou 1996; Peacock 1997). The second method calculates the ratio of the quadrupole to monopole moments of the redshift space power spectrum (see Hamilton 1993a,1995,1997a; Bromley 1994; Fisher *et al.* 1994; Cole, Fisher, & Weinberg 1994,1995; Lin 1995; Fisher & Nusser 1996; Taylor & Hamilton 1996; Bromley, Warren, & Zurek 1997). The third utilizes a maximum likelihood approach in which the amplitudes of individual modes, β, and the power spectrum are taken as parameters of the model (see Fisher, Scharf, & Lahav 1994; Heavens & Taylor 1995; Ballinger, Heavens, & Taylor 1995). An excellent review of these methods along with a thorough background of the linear redshift distortion problem is given in Hamilton (1997a).

Other work dealing primarily with the development of new methods, theoretical analysis, and constraints on surveys can be found in Lahav *et al.* (1991); Suto, & Suginohara (1991); Hamilton (1992,1993b,1997); Gramann, Cen, & Bachall (1993); Gramann, Cen, & Gott (1994); Hamilton & Culhane (1996); Matsubara, & Suto (1996); Zaroubi, & Hoffman (1996); de Laix & Starkman (1998); Szalay, Matsubara, & Landy (1998); Hatton & Cole (1998,1999); and Nakamura, Matsubara, & Suto (1998).

In more recent work, Tadros *et al.* (1999) present a spherical harmonic analysis of the linear distortions in the PSCz Galaxy Catalog and include a detailed synopsis of many of the linear distortion measurements listed above. They measure $\beta = 0.58 \pm 0.26$. In Matsubara, Szalay, & Landy (2000), the first application of the Karhunen-Love (K-L) eigenmode compression technique to this problem is presented using the Las Campanas Redshift Survey data with an estimation of $\beta = 0.30 \pm 0.39$. Hamilton, Tegmark, & Padmanabhan (2000) analyze the PSCz catalog also using a K-L expansion technique and determine $\beta = 0.41^{+0.13}_{-0.12}$. A modified approach incorporating eigenvectors is described in Taylor *et al.* (2001) who find $\beta = 0.39^{+0.14}_{-0.12}$. Ratcliffe *et al.* (1998) using the Durham/UKST Galaxy Redshift Survey estimate $\beta \sim 0.5$. Peacock *et al.* (2001), using over 141,000 galaxies from the Two-Degree Field Survey report a value of $\beta = 0.43 \pm 0.07$ using a two parameter model of the distortions in the redshift space correlation function. Tegmark, Hamilton, & Xu (2000) apply a pseudo K-L eigenmode analysis to the Two-Degree Field public release data and estimate $\beta = 0.49 \pm 0.16$.

3. Removing the Distortions

All of the methods listed above depend upon a measurement of the distortion signal, subject to all its complexities. However, Kaiser's identification of the redshift distortions with a statistically equivalent distortion of the real space mass density presents another approach to the problem. In Tegmark & Bromley (1995), an analytical reconstruction of a real space density field from a redshift space density field, such as that derived from a redshift survey, was described. However, as with attempts to model the distortions, the procedure had a complicated functional form and involved a relatively high dimensional integral. Because of this, it was suggested that such as inversion was best handled by parallel computation on a supercomputer. Setting computational complexities aside, the reconstruction of the real space density field presents a powerful new approach to this problem.

As previously discussed, a direct fit of a model to either the correlation function or power spectrum in redshift space presents numerous difficulties due to the fundamental complexity of the effects of the distortions. Additionally, many of these methods include assumptions concerning either the underlying power spectrum or correlation function on large linear scales. However, rather than measuring the distortions themselves, another approach would be to invert the density enhancements and statistically re-create the real space density field. Since two-point estimators such as the power spectrum and correlation function are statistical anyway, one could invert the density field and simply search for the value of β that results in a symmetric function. In other words, when the field is properly inverted the anisotropies disappear.

This method would work as follows:

1) Take the data and perform the inversion for different values of the redshift distortions as parameterized by β.
2) For each of these inversions, calculate the power spectrum or correlation function that results from the inverted data.
3) Look for the appropriate symmetry in the resulting function.

Here the problem is reduced from the having to calculate and fit a very complex function with an assumed power spectrum, to applying an inversion technique to the data itself and looking for a symmetric signal.

3.1. A Novel Method for Removing the Distortions

Consider again Kaiser's analysis of the redshift space distortions. The power of his approach resulted from considering a plane wave density fluctuation in real space. As shown above, this fluctuation maps to redshift space as

$$\Delta_s(\mathbf{r}) = \Delta_r(\mathbf{r})(1 + \beta\mu^2) \tag{6}$$

where $\mathbf{r}$ the line-of-sight in either real or redshift space. This relation is easily inverted to first order to give the real space density fluctuation,

$$\Delta_r(\mathbf{r}) = \frac{\Delta_s(\mathbf{r})}{1 + \beta\mu^2}. \tag{7}$$

At first this development may seem academic in that redshift surveys do not appear to consist of plane wave density fluctuations. However, a redshift survey consists of a collection of galaxies, which for all intents and purposes can be considered point particles. As point particles, it is simple to construct a δ-function plane wave expansion of each individual point. Since each point has a well-defined position vector, it is easy to calculate the *undistortion* coefficient $1/(1+\beta\mu^2)$ for each wavevector in the expansion for a given β. Once this is done, the real space density can be reconstructed by re-summing this same set of plane waves with their modified amplitudes.

Mathematically, the procedure is very straightforward. The real space mass density $\rho(\mathbf{r})$ at any point $\mathbf{r}$ is given by

$$\rho(\mathbf{r}) = \frac{1}{n}\sum_{i=1}^{Ngal}\sum_{j=1}^{n}\left(\frac{1}{1+\beta\mu_{ij}^2}\right)\exp[\mathrm{i}(\mathbf{k_j}\cdot\mathbf{r} - \mathbf{k_j}\cdot\mathbf{r_i})]. \tag{8}$$

Here each galaxy i at position $\mathbf{r_i}$ is expanded in a δ-function plane wave expansion over a set of n wavevectors $\mathbf{k_j}$, the amplitude of each wavevector is divided by the inversion coefficient, $1 + \beta\mu_{ij}^2$ where $\mu_{ij} = \cos(\hat{\mathbf{k}}_\mathbf{j}\cdot\hat{\mathbf{r}}_\mathbf{i})$, the sum taken over all galaxies and the density reconstructed at $\mathbf{r}$. Given the rotational but not translational invariance of these distortions, it is fortunate that the inversion of this problem can be expressed so simply in Cartesian coordinates using the Fourier transform.

In practice this procedure is only slightly more complicated than that described above. The complications have to do with accounting for survey geometry, taking into account the non-linear small-scale pairwise distortions, choosing a finite set of wavevectors to expand over, and developing a sensitive method for determining when the β distortions have been removed.

4. Testing the Method

To develop and test the method, numerical simulations were used (see Cole *et al.* 1999). Simulations are very convenient since the parameters of the 'data' are known and real space positions of the galaxies are also available. To make the procedure computationally efficient, the analysis was restricted to thin slices of simulated data 2° thick by 55° wide by 200 to 500 h^{-1}Mpc deep. Each slice contained approximately 5000 galaxies and the radial selection function was modeled after that of the SDSS. As an initial test, simulation data spanning four different cosmologies were used: two Cobe normalized models with $\beta = 0.57$ ($\Omega_m = 0.5$), $\beta = 0.26$ ($\Omega_m = 0.3$), one tilted-flat model with $\beta = 0.51$ ($\Omega_m = 1.0$), and two independent τCDM flat models with $\beta = 0.54$ ($\Omega_m = 1.0$). These are named O3, O5, E2, and E3SA, E3SB in Cole *et al.* (1999), respectively.

Central to the method is to first expand the data in a Fourier expansion. Each point must be expanded and the new Fourier amplitudes calculated individually since the distortions depend upon $\cos(\hat{\mathbf{k}} \cdot \hat{\mathbf{r}})$. In computing the Fourier expansion, the data was binned with a resolution $1h^{-1}$Mpc using a grid of 1024×1024 in two dimensions and a FFT performed. By using very thin slices, the expansion could be carried out in two rather than three dimensions, limiting the computational effort. Further work will efficiently adapt this method to three dimensions. On this scale in two dimensions there are already 512×1024 amplitudes that must be calculated.

After all amplitudes have been modified, their Fourier amplitudes are added back together and an inverse FFT performed. This operation returns the undistorted density field. The field is then cut to correspond to the geometry of the original slice. This procedure was carried out for twenty slices and the $\xi_z(r_p, \pi)$ correlation function calculated for each one. All twenty correlation functions were averaged together to construct the mean. The mean correlation function was then windowed with a Hann window with a limit of $64h^{-1}$Mpc and Fourier transformed. This returned the power spectrum of the $\xi_z(r_p, \pi)$ decomposition.

Although the focus of this method is to measure β, as was shown in Figure 1, $\xi_z(r_p, \pi)$ also contains small-scale pairwise velocity distortions in the non-linear regime. These distortions have been shown to be well-characterized by an exponential distribution, which is equivalent to a Lorentzian distortion in the power spectrum (see Landy, Szalay & Broadhurst 1998; Landy 2002). The full distortion function of the power spectrum is given by the ratio

$$\frac{P_s(k)}{P_r(k)} = \frac{(1 + \beta\mu^2)^2}{1 + \frac{1}{2}k^2\mu^2\sigma_{12}^2(k)} \tag{9}$$

where $\sigma_{12}/\sqrt{2}$ is the decay width of the exponential. Using simulated data, it is simple to construct this ratio by dividing the power spectrum of the redshift space data by that of real

space data. The ratio of these power spectra is shown in Figure 2. The coordinate system is the Fourier analogue of the (r_p, π) basis and is denoted by (k_{r_p}, k_π).

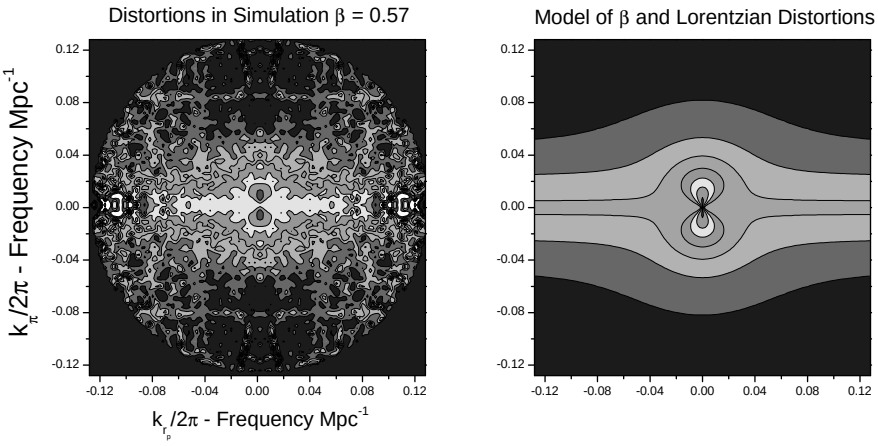

Fig. 2.— *The left panel shows the distortions in the power spectrum for the simulated data. This was constructed by dividing the power spectrum in redshift space by the power spectrum in real space, using the real and redshift space functions from the simulated data. On the right is an analytical representation of the same function with* $\beta = 0.57$ *and* $\sigma_{12} = 360$ *km/sec. The agreement between the analytical model and the distortions is quite good. The 'bubble' in the center (long wavelengths) shows the linear infall distortions. The distortions across the graph are due to the small-scale pairwise velocity dispersion function (the Lorentzian).*

As shown in Figure 2, most of the signal from the β distortions is found near the core. However, since the β and small-scale distortions are competing effects, systematic errors will result if the small-scale distortions are not modeled correctly, especially at larger scales (in the core), and these errors will be positively correlated. A method to overcome the problem of modeling the small-scale distortions is described below.

4.1. Removing the Distortions from Redshift Space Data

To test the method, the procedure described above was used to remove the β distortions from the redshift space data. In practice, the distorted data was smoothed on 8 mpc scales and the correlation function windowed at 64 mpc to limit noise. Figure 3 shows the original smoothed and windowed power spectrum, and the power spectra for three values of β used to remove the distortions.

Due to the residual non-linear distortions, the end result of this procedure is not expected to be a circularly symmetric function. However, the non-linear distortions effectively act only in the k_π direction, that is along the line of sight. Therefore, even when the β distortions

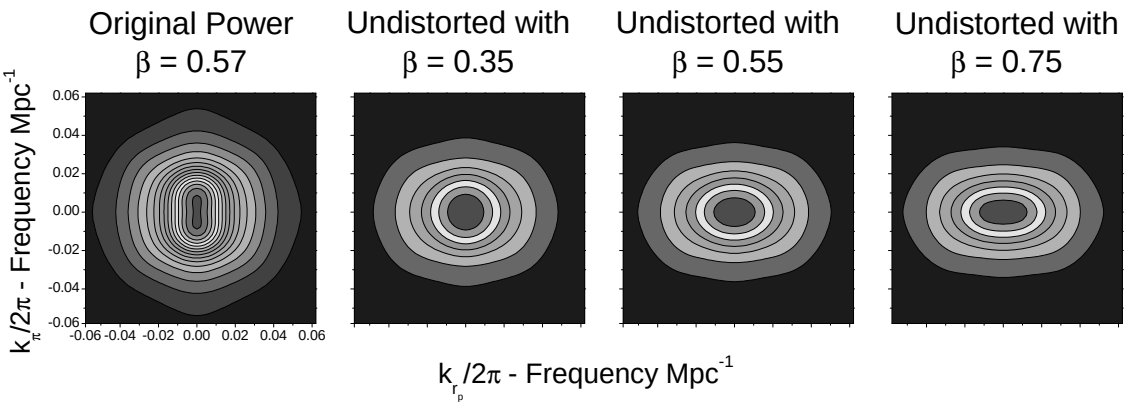

Fig. 3.— *The original power spectrum, and the power spectra for three sample values of* β *used to remove the distortions for the* $\beta = 0.57$ *simulation. Although the case of* $\beta = 0.35$ *appears to be the most symmetric result, the small scale non-linear distortions have not yet been taken into account. As will be shown in Figure 4, the vertically compressed signal of* $\beta = 0.55$ *is actually very close to the expected result.*

have been completely removed what is expected is a vertically compressed function about the k_{r_p} axis.

What is needed at this stage is a method to account for the non-linear distortions. One of the fundamental challenges of any method is in trying to simultaneously fit the β and non-linear distortions. The main problem derives from the situation that these distortions are competing effects and their errors are positively correlated.

To overcome this difficulty, a procedure was developed to estimate the non-linear distortions from the data itself, taking advantage of only the geometrical knowledge of how they effect the power spectrum. This also belies any problem which might arise from smoothing and windowing the data before transforming.

In theory, neither the β nor the non-linear distortions effect the power along the k_{r_p} axis, so the power along this axis can be utilized as the model underlying power spectrum. Additionally, if the β distortions have been removed in their entirety, the only remaining signal should be due to the residual non-linear distortions, which should be independent of k_{r_p}. Figure 4 shows the power spectrum of the data divided by the expected power as a function of $|k|$, given by the signal along the k_{r_p} axis. The power is almost perfectly symmetrical and independent of k_{r_p} axis about the k_{r_p} axis near the correct value of $\beta = 0.57$. Either under-correction using $\beta = 0.35$ or over-correction using $\beta = 0.75$, leave obvious signatures in the result.

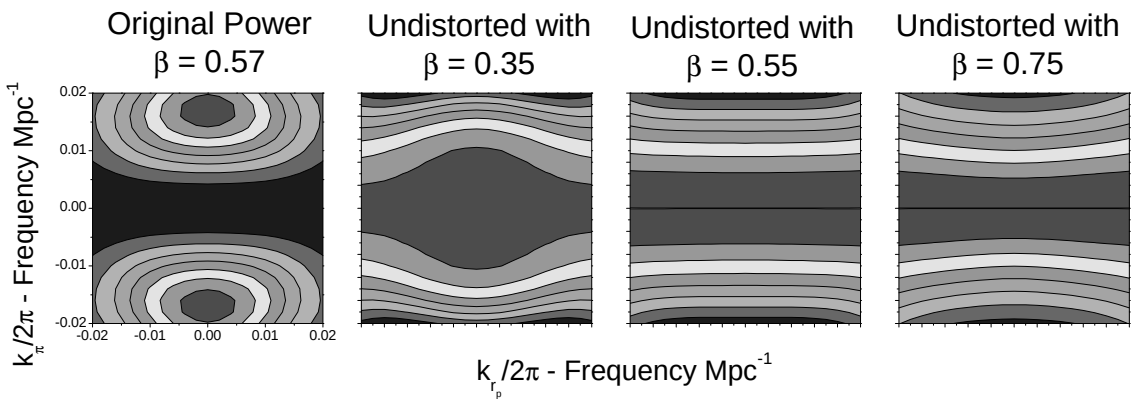

Fig. 4.— *The original power spectrum and that for three sample values of β used to remove the distortions divided by the model power spectrum as derived from the data (the value along the k_{r_p} axis). If the β distortions have been correctly removed, this function should be symmetric about the k_{r_p} axis. The cases for $\beta = 0.35$ and $\beta = 0.75$ clearly show under and over corrections.*

4.2. A Sensitive Fit

The ratios shown in Figure 4 illustrate the utility of the technique. To actually determine the best fit value of β, however, the numerical difference between the intrinsic model derived from the data, that is the signal along the k_{r_p} axis, and the undistorted spectra for different values of β was used. From this, a generalized 'chi-square' function was calculated to determine the optimal value of β. Figure 5 shows this difference function for several values of β although over a much smaller range to illustrate the sensitivity of this method.

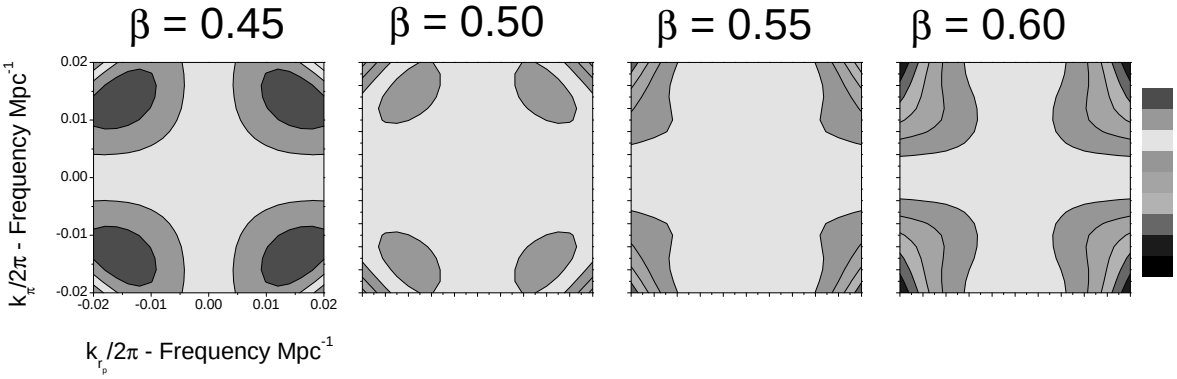

Fig. 5.— *The difference between four sample values of β and the underlying power derived from the signal along the k_{r_p} axis. Here a much smaller range in β was used in order to show the sensitivity of the method. The inversion of the differences is due to the different phase of under and over-corrections.*

Figure 6 shows the 'chi-square' values for the appropriate β using four cosmologies and five simulations. This chi-square is simply the sum of the squares of the difference functions shown in Figure 5, normalized by dividing each by its minimum value for ease of comparison. The function was calculated inside a central ring of radius of $k/2\pi = 0.02$, corresponding to wavelengths greater than or equal to 50 mpc. The sampling resolution of the difference function is $\Delta k/2\pi = 0.002$.

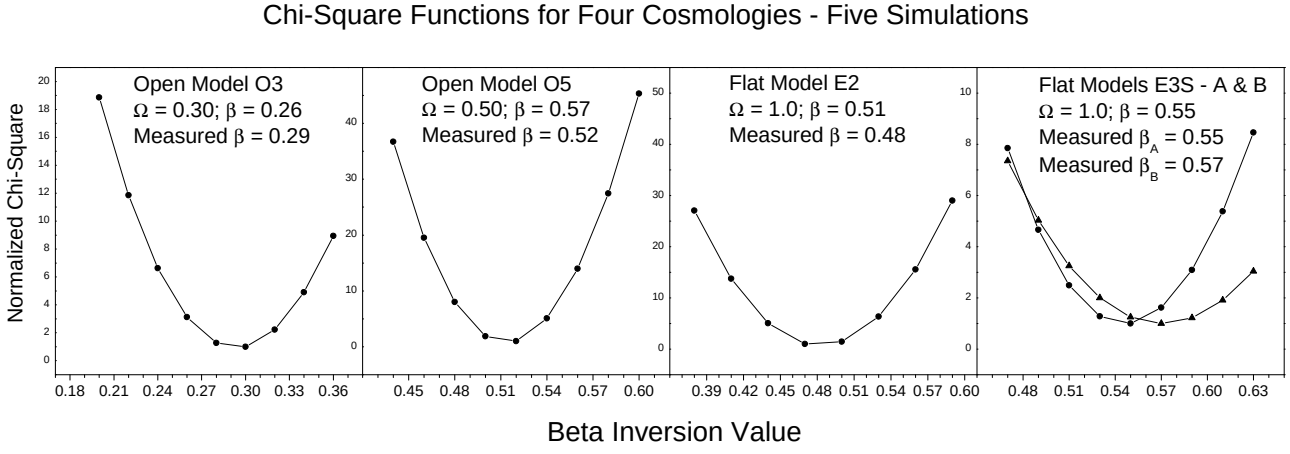

Fig. 6.— *Chi-square functions for the method using CDM simulations with* $\beta = 0.26$ *(*$\Omega_m = 0.3$*),* $\beta = 0.57$ *(*$\Omega_m = 0.5$*),* $\beta = 0.51$ *(*$\Omega_m = 1.0$*), and* $\beta = 0.54$ *(*$\Omega_m = 1.0$*). These include COBE, structure normalized, and mixed models. The uncertainty in* β *across these results is* ± 0.031*. For more detail on the simulations see the text and Cole et al. (1999).*

The results include a COBE normalized open $\beta = 0.26$ ($\Omega_m = 0.3$) model and a COBE normalized open $\beta = 0.57$ ($\Omega_m = 0.55$) model, a mixed COBE and structure normalized flat $\beta = 0.51$ ($\Omega_m = 1.0$) model, and two independent structure normalized flat $\beta = 0.54$ ($\Omega_m = 1.0$) models. Across these models, β has been measured to an uncertainty of ± 0.031. The errors in the estimates are not systematically high or low across the simulations. This compares favorably to the recent Two-Degree Field result of $\beta = 0.43 \pm 0.07$ (see Peacock *et al.* 2001), where the uncertainties are over a factor of two higher.

4.3. Difficulties in Applying the Method to Current Survey Data

Although in theory this method is very straightforward, in practice the idiosyncracies of real survey data present other challenges. Fortunately, these difficulties will disappear once the surveys become more contiguous, as they result from the complexity of current survey geometries.

For the technique to be applied successfully, it is necessary to be able to break up the survey into thin slices of fairly contiguous data, which do not include a large number of voids or holes. If there exist a large number of edges in the data due to a complex angular selection function, then the undistorted signal will leak out across the edges and into the geometrical voids in the survey when the data is inverted. This signal is then removed from the data when the geometric angular selection function cuts are made. This difficulty is not unexpected when considering that most of the distortion signal comes from scales above 30 h^{-1}Mpc, and if the data is not contiguous on these scales, then the signal will be lost. To improve the method, experiments are underway to efficiently expand the method to three dimensions to circumvent this problem.

5. Conclusion

A method for determining the value of $\beta = \Omega_m^{0.6}/b$ based upon a Fourier inversion of distortions in the redshift space density field has been presented. In contrast to many other measures, this technique does not rely on a complex modeling of the expected distortions in the redshift space correlation function or power spectrum. Instead by inverting the redshift space density distortions as parameterized by β, it is possible to fit for a symmetric signal in the redshift space power spectrum. This technique is not dependent on the small angle/plane-parallel approximation and can make full use of large redshift survey data. The only present difficultly with this method is that it does depend on data that is fairly contiguous on large scales. Such data should become available from large redshift surveys within the next few years. It has been tested using simulations with four different cosmologies and returns the value of β to ± 0.031, greater than a factor of two improvement over existing techniques. Presently, it has been tested in two-dimensions using thin slices of data to limit the computational burden, but can easily be expanded to three-dimensions.

6. Acknowledgements

The authors would like to thank S. Cole, S. Hatton, D.H. Weinberg, and C. S. Frenk (1999) for the use of their simulation data, which they have made easily accessible to the astronomical community. S. Landy acknowledges support from the Jeffress Memorial Trust and NSF Grant AST 99-00835. A. Szalay acknowledges support from ...

REFERENCES

Ballinger, W. E., Heavens, A. F., & Taylor, A. N. 1995, MNRAS, 276, L59

Baugh, C. M. 1996, MNRAS, 280, 267

Bromley, B. C. 1994 ApJ, 423, L81

Bromley, B. C., Warren, M. S., & Zurek, W. H. 1997, ApJ, 475, 414

Cole, S., Hatton, S., Weinberg, D. H., Frenk, C. S. 1999, MNRAS, 300, 945

Cole, S., Fisher, K. B., & Weinberg, D. H. 1994, MNRAS, 267, 785

Cole, S., Fisher, K. B., & Weinberg, D. H. 1995, MNRAS, 275, 515

de Laix, A. A., & Starkman, G. 1998, ApJ, 501, 427

Fisher, K. B., Davis, M., Strauss, M. A., Yahil, A., & Huchra, J. P. 1994, MNRAS, 267, 927

Fisher, K. B., & Nusser, A. 1996, MNRAS. 275, L1

Fisher, K. B., Scharf, C. A., & Lahav, O. 1994, MNRAS, 266, 219

Fry, J. N., & Gaztañaga, E. 1994, ApJ, 425, 1

Gramann, M., Cen, R., & Bachall, N. A. 1993, ApJ, 419, 440

Gramann, M., Cen, R., & Gott, R. J. III. 1994, ApJ, 425, 382

Hamilton, A. J. S. 1992, ApJ, 385, L5

Hamilton, A. J. S. 1993a, ApJ, 406, L47

Hamilton, A. J. S. 1993b, ApJ, 417, 19

Hamilton, A. J. S. 1995, in IRAS Surveys, Clustering in the Universe, Proc. XVth Recontres de Moriond, ed. Maurordato *et al.* , Editions Frontières, 143

Hamilton, A. J. S. 1997a, in The Evolving Universe 1996, ed. Hamilton, D. (Dordrecht: Kluwer Academic), 185

Hamilton, A. J. S. 1997b, MNRAS, 289, 295

Hamilton, A. J. S., & Culhane, M. 1996, MNRAS, 278, 73

Hamilton, A. J. S., Tegmark, Max, Padmanabhan, N. 2000, MNRAS, 317, L23

Hatton, S. J., & Cole, S. 1998, MNRAS, 296, 10

Hatton, S. J., & Cole, S. 1999, MNRAS, 310, 1137

Heavens, A. F., & Taylor, A. N. 1995, MNRAS, 275, 483

Kaiser, N. 1987, MNRAS, 227, 1

Lahav, O., Lilje, P. B., Primack, J. r., & Rees, M. J. 1991, MNRAS, 251, 128

Landy, S. D. 2002, ApJ, 567, L1

Landy, S. D., Szalay, A. S., & Broadhurst, T. J. 1998, ApJ, 494, L133

Lin, H. 1995, The Las Campanas Redshift Survey, PhD Thesis, Ch. IV

Loveday, J., Efstathiou, G., Maddox, S. J., & Peterson, B. A. 1996, ApJ, 468, 1

Matasubara, T., Szalay, A. S., & Landy, S. D. 2000, ApJ, 535, L1

Matsubara, T., & Suto, Y. 1996, ApJ, 470, L1

Nakamura, T. T., Matsubara, T., & Suto, Y. 1998, ApJ, 494, 13

Peacock, J. A. 1997, MNRAS, 284, 885

Peacock, J. A., & Dodds, S. J. 1994, MNRAS, 267, 1020

Peacock, J. A. *et al.* 2001, Nature, 410, 169

Peebles, P. J. E. 1980, The Large Scale Structure of the Universe (Princeton:Princeton University Press)

Ratcliffe, A., Shanks, T., Parker, Q. A., & Fong, R. 1998, MNRAS, 296, 191

Sargent, W. L. W., & Turner, E. L. 1977, ApJ, 212, L3

Suto, Y., & Suginohara, T. 1991, ApJ, 370, L15

Szalay, A. S., Matsubara, T., & Landy, S. D. 1998, ApJ, 498, L1

Tadros, H., & Efstathiou, G. 1996, MNRAS, 282, 1381

Tadros, H., Ballinger, W. E., Taylor, A. N., Heavens, A. F., Efstathiou, G., Saunders, W., Frenk, C. S., Keeble, O., McMahon, R., Maddox, S. J., Oliver, S., Rowan-Robinson, M., Sutherland, W. J., & White, S. D. M. 1999, MNRAS, 305, 527

Taylor, A. N., & Hamilton, A. J. S. 1996, MNRAS, 282, 767

Taylor, A. N., Ballinger, W. E., Heavens, A. F., & Tadros, H. 2001, MNRAS, 327, 689

Tegmark, Max, & Bromley, B. C. 1995, ApJ, 453, 533

Tegmark, Max, Hamilton, A. J. S., & Xu, Y. 2001, MNRAS, submitted

Zaroubi, S., & Hoffman, Y. 1996, ApJ, 462, 25